Journal of Applied Polymer Science

Antiscaling Properties of Novel Maleic-Anhydride Copolymers Prepared via Iron (II) – Chloride Mediated ATRP

Yousef M. Al-Roomi, Kaneez F. Hussain
Chemical Engineering Department, Kuwait University, 13060 Safat, Kuwait
Correspondence to: Y. M. Al-Roomi (E-mail: yalroomi@kuc01.kuniv.edu.kw)

ABSTRACT: A class of maleic anhydride copolymers (YMR-A series) with a narrow molecular weight distribution between 500–1500 and a polydispersity of 1.0–1.11 was obtained from n-alkylacrylamide and maleic anhydride monomers via atom transfer radical polymerization. The monomer conversion reached about 71% corresponding to 1:4 [$FeCl_2$] to [SA] molar ratios for (AAH/MA) copolymer initiated by CPN whereas for the polymerization initiated by MCPN the conversion reached 51.9% under similar condition showing better performance of CPN initiator. Resultant polymers were characterized by means of ^{1}H-NMR and ^{13}C-NMR. The inhibition behavior of these YMR-A polymers against $CaCO_3$ and $CaSO_4$ was evaluated using static scale inhibition method. The inhibition efficiency on the calcium carbonate scale is much higher and even with 5 ppm dosage level the efficiency is around 99.33 % at pH 10.45 and temperature 70°C, where as for calcium sulfate scales the inhibition efficiency, is lower and 99.9% inhibition is observed at 7–9 ppm level. © 2013 Wiley Periodicals, Inc. J. Appl. Polym. Sci. **2014**, *131*, 39827.

KEYWORDS: applications; kinetics; properties and characterization; copolymers

Received 20 March 2013; accepted 6 August 2013
DOI: 10.1002/app.39827

INTRODUCTION

In water treatment and water desalination processes scale formation has been recognized as a widespread problem.[1,2] The precipitation of scaling salts such as $CaSO_4$ and $CaCO_3$ on membranes leads to significant water flux decline.[3–7] Many different synthetic water-treatment polymers have been employed in a wide range of water treatment application as dispersants for particulate matter, inhibitors of mineral scale formation and deposition, and corrosion inhibitors.[8–11]

It is a well known fact that the polymers which are effective anti-precipitants and de-scalants are of relatively low molecular weight, i.e., below 10,000[6,12–14] and preferably in between 500 and 4000.[15–21] Polymers are generally of low molecular weight to prevent bridging of suspended solids, but of sufficient structure to adhere to developed scale formation i.e., they can be adsorbed onto the active growth sites of the crystal surface, and disturb the regular outgrowth of $CaCO_3$ or $CaSO_4$ crystal.[22,23]

Maleic acid-based polymers are particularly effective in the desalination of seawater by the multi-stage flash evaporation (MSF).[24–27] Their action is enhanced when maleic acid is co-polymerized with a small proportion of other monomers, such as acrylates. This has already been proved by the low molecular weight YMR-polymers synthesized in our laboratory by free radical mechanism[28,29] which shows high scale inhibition efficiency.[30] Therefore main aim of this work is to further synthesize such polymers using maleic anhydride with different acrylates which shows better antiscalant performance and to study the scale inhibition performance of these synthesized polymers.

Atom transfer radical polymerization (ATRP) is today one of the most effective protocols available for achieving controlled/living radical polymerizations of a range of monomers, and it is used in the mass production of various well-defined polymers with controlled topology and functionality.[31–34]

The key for successful ATRP is to employ proper catalytic system with high activity and selectivity. Recently iron-based catalysts have attracted a particular attraction, because of their low toxicity, low cost, and biocompatibility. According to published reports, various iron (II) complexes, such as $FeBr_2$/trialkylamine,[35] $FeCl_2$/α-dimine,[36] $FeCl_2$/tridentate salicylaldiminato,[37] $FeCl_2$/tridentate nitrogen ligands,[38] $FeCl_2$/tetradentate nitrogen ligands,[39] $FeCl_2.4H_2O$/hexamethylphosphoric triamide,[40] and FeX_2/DPPMP[41] were active catalysts for the living radical polymerization.

Designing new ligands that are cheaper and more easily available and show better catalytic behavior has become an important research area in ATRP. The choice of ligand is one of the key factors influencing the reactivity of catalyst. Acids which are inexpensive and nontoxic complex more easily with iron than

© 2013 Wiley Periodicals, Inc.

with copper and may therefore act as a ligand in iron-mediated ATRP. A new catalytic system, based on iron complexes with succinic acid (SA) has been studied by Hou et al.[42] for the ATRP of acrylonitrile. Therefore in our present study we have studied this catalytic system for controlled/living polymerization of maleic anhydride with various substituted n-alkyl acryl amides. The influence of ratio of the metal to ligand has also been investigated. Besides static scale inhibition method is used to evaluate the inhibition performance.[43–46]

EXPERIMENTAL

Materials

Maleic anhydride (Sigma, 99 %) was recrystallized from reagent grade benzene and dried under vacuum at room temperature. *N*-propyl amine (Sigma, 98 %), n-butyl amine (Fluka, 99 %), n-hexyl amine (Merck, 98 %), benzamide (Merck, 98 %), methyl-2-chloropropionate (Merck, 98 %), 2-chloropropionitrile (Aldrich, 95 %), $FeCl_2$ (Himedia, 98 %), succinic acid (Fluka, 99 %), and acrolyl chloride (Fluka, 96 %) were used without further purification. Solvent tetrahydrofuran (THF) used for spectroscopic measurements was of spectral grade (Fluka) and was used as received.

All the chemicals for inhibition efficiency tests were reagent grade and the brines were prepared as per the standard NACE TM 0374-95.

Instrumental Measurements

Molecular weight measurements of the monomers and copolymers were carried out by high temperature size exclusion chromatography (SEC) using a Waters 150C ALC/GPC system. ^{1}H-NMR spectra and ^{13}C-NMR spectra were obtained using a Bruker AM 400 NMR spectrometer. The samples were dissolved in $CDCl_3$ or acetone-d_6 and the shifts were referenced to tetramethylsilane.

Copolymerization of Maleic Anhydride

Monomer Synthesis. Substituted amine (n-alkyl amines/benzamide) and barium hydroxide (w/w; 1 %) were placed in the 200 mL round bottom flask placed in an ice bath and stirred until the temperature equilibrated. Acrolyl chloride was added drop wise to the flask with continuous stirring till the reaction mixture thickened indicating the formation of the monomer. The reaction mixture was then heated gradually up to 85°C, until hydrogen chloride was eliminated. The resulting solution was whitish-yellow and turbid. Doubly deionized water or water $CHCl_3$ mixture (1:3) was added to the vessel with vigorous stirring to separate the monomer. The resulting material was dried by placing it in a 40°C oven. The final product was then stored at 0°C. Similarly four different monomers i.e. N-Propylacrylamide (AAP), N-Butylacrylamide (AAB), N-Hexylacrylamide (AAH) and N-Acryloylbenzamide (ABA) were synthesized.

Copolymerization. Copolymerization of MA with n-alkylacrylamide monomers was conducted at 5:5 monomer ratios in o-xylene using a $FeCl_2$/SA catalyst system initiated by 2-chloropropionitrile (CPN) or methyl-2-chloro-propionate (MCPN). The contents were purged with N_2 to eliminate O_2 for ~15 min. The reaction was conducted at three different molar ratios of [monomers] / [initiator] / [$FeCl_2$] / [SA], i.e. (100:1:1:1), (100:1:1:2) and (100:1:1:4), respectively. The temperature of the reaction was maintained at 140°C. The progress of the reaction was followed by measuring the disappearance of the monomer, which was conducted by taking out a small sample of reaction mixture every hour and determining its monomer content by LC and increase in molecular weight of the polymer by gel permeation chromatography.

A typical polymerization was carried out as follows. MA, n-substituted alkyl acryl amide, $FeCl_2$ and SA dissolved in 200 mL of o-xylene was stirred and heated under a N_2 atmosphere until the temperature reached 70°C. Initiator (CPN / MCPN) dissolved in 50 mL of solvent were added over a period of 30 min. Refluxing was continued for a further 10 h and the polymer was allowed to separate from the solution. Excess of solvent was distilled off and the oily layer so obtained was recrystallized in appropriate solvent to give the copolymer product.

RESULTS AND DISCUSSION

It is obvious from our previous work[30] that low molecular weight copolymers of MA have been quite effective as scale inhibitors. Therefore this present work is targeted in the synthesis of such low molecular weight polymers and reports the copolymerization of MA with varying substituted n-alkyl acrylamides. Besides, the main focus is the ATRP process in copolymerization of substituted alkylacrylamides with maleic anhydride, which is believed to be difficult to polymerize and produce low molecular weight polymers with narrow polydispersities. Although many studies have been based on copper mediated ATRP, iron based ATRP studies are relatively scarce. Therefore present work aims at studying a new catalytic system based on iron complexes with succinic acid.

Copolymerization of maleic anhydride with n-substituted acryl amide was carried out in both polar solvent (DMF) and nonpolar solvent (toluene, o-xylene and THF); however, more positive results were obtained in nonpolar solvents. Polymerization in THF and DMF yielded a dark oily substance, which was difficult to purify. A very low conversion was obtained in toluene. Maleic anhydride polymerized effectively in o-xylene. Therefore all the polymerization was conducted in o-xylene at 140°C. Other temperatures 110°C and 120°C were also tried but a very low conversion was obtained.

Therefore we have focused mainly on the reaction proceeding at 140°C, in o-xylene at 5:5 monomer ratio using the $FeCl_2$/SA catalyst system initiated by 2-chloropropionitrile (CPN) or methyl-2-chloro-propionate (MCPN). The reaction is conducted at three different molar ratios of [monomers]/[initiator]/[$FeCl_2$]/[SA], i.e. (100:1:1:1), (100:1:1:2), and (100:1:1:4) respectively (Tables I and II).

Characterization of Synthesized Copolymers

The YMR-A series, maleic anhydride copolymers were analyzed by ^{1}H-NMR and ^{13}C-NMR spectroscopy.[29,47,48] In the proton NMR-spectra for the copolymers, the protons were indexed starting from the initiator denoted as "I" (2-chloropropionitrile or methyl-2-chloropropionitrate radical) as shown in Figures 1(a–c). Signals between 0.8 and 1.5 ppm can be attributed to

Table I. Conditions and Results for the ATRP Copolymerization of MA Initiated by CPN in o-Xylene at 140°C

Run	Scale inhibitors	Monomers		CPN/$FeCl_2$/SA	Conversion (%)	$M_{n\ GPC}$	M_w/M_n	k_{app}[a] (S^{-1})
1	YMR 140-A	MA	AAH	1 : 1 : 1	66.6	853	1.08	1.6×10^{-3}
2	YMR 141-A	MA	AAH	1 : 1 : 2	67.35	871	1.02	1.7×10^{-3}
3	YMR 142-A	MA	AAH	1 : 1 : 4	71	1466	1.00	1.9×10^{-3}
4	YMR 145-A	MA	AAB	1 : 1 : 1	44.66	500	1.06	0.9×10^{-3}
5	YMR 143-A	MA	AAB	1 : 1 : 2	47.14	580	1.09	1×10^{-3}
6	YMR 144-A	MA	AAB	1 : 1 : 4	67.14	1215	1.07	1.7×10^{-3}
7	YMR 146-A	MA	AAP	1 : 1 : 1	38.66	610	1.09	0.7×10^{-3}
8	YMR 147-A	MA	AAP	1 : 1 : 2	45.9	628	1.10	0.9×10^{-3}
9	YMR 148-A	MA	AAP	1 : 1 : 4	53.84	852	1.09	1.2×10^{-3}
10	YMR 161-A	MA	ABA	1 : 1 : 1	27.87	533	1.04	0.5×10^{-3}
11	YMR 160-A	MA	ABA	1 : 1 : 2	29.68	535	1.06	0.6×10^{-3}
12	YMR 149-A	MA	ABA	1 : 1 : 4	50	598	1.06	1×10^{-3}

[a] k_{app}, the slope of $\ln[M_o]/[M]$ versus time plot.

aliphatic protons [H_i – H_h] of the alkyl acryl amide group. The methene proton [H_d] gives a duplex in the range 2.2–2.8 ppm. The methylene proton [H_g] near the amide group and proton [H_b] and [H_c] of the maleic anhydride group give peaks at 3.35–3.7 ppm. The methene proton of the nitrile group and methene proton [H_e] give a comlex pattern between 5.7 and 6.7 ppm. Finally a singlet around 7.2 ppm can be assigned to the –NH proton [H_f].

The proton NMR spectrum for the benzamide copolymer [Figure 1(d)] shows a singlet at 2.7 ppm due to the methyl group of the 2-chloropropionitrile / methyl-2-propionate radical. The proton [H_c] of the maleic anhydride group, proton [H_b] and proton [H_f] give peaks at 3.74–3.78 ppm. The methene proton [H_d] of the maleic anhydride group gives triplet between 2.84 and 2.87 ppm. A complex pattern is observed between 6.5 and 7.8 ppm due to the benzene ring [H_g] of the benzamide group. Finally a singlet is observed at 7.8 ppm due to –NH proton [H_g].

^{13}C-NMR spectra of the copolymers are shown in Figure 2. Peaks in the spectra are divided into four groups. The first group (I) from 12 - 41 ppm, second group (II) from 76 to 79 ppm, third group (III) from 127 to 134 ppm and the final group (IV) from 165 to 173 ppm. The first group (14–41 ppm) is attributed to the methyl and methylene groups of the alkyl unit. The peaks located at 76–79 ppm correspond to the vinyl group of the acryl amide unit and MA (Cα of the carbonyls in both the cases). Peaks located between 124 and 136 ppm are due to the nitrile group of the 2- chloropropionitrile radical. The carbonyls in the maleic anhydride and amide group give peaks between 165 and 173 ppm. The ^{13}C-NMR spectrum of benzamide copolymer [Figure 2(d)] is also divided in four groups as above. The first group between 28 and 38 ppm is attributed to the aliphatic group of the 2-chloropropionitrile/ methyl-2-chloropropionate group and methene carbon of maleic anhydride. The peaks located at 67–79 ppm correspond to the vinyl group of acryl amide unit and due to solvent

Table II. Conditions and Results for the ATRP Copolymerization of MA Initiated by MCPN in o-Xylene at 140°C

Run	Scale inhibitors	Monomers		CPN/$FeCl_2$/SA	Conversion (%)	$M_{n\ GPC}$	M_w/M_n	k_{app}[a] (S^{-1})
1	YMR 155-A	MA	AAH	1 : 1 : 1	41.35	530	1.11	0.8×10^{-3}
2	YMR 153-A	MA	AAH	1 : 1 : 2	45	863	1.07	0.9×10^{-3}
3	YMR 154-A	MA	AAH	1 : 1 : 4	51.89	1280	1.06	1.1×10^{-3}
4	YMR 150-A	MA	AAB	1 : 1 : 1	42.1	566	1.08	0.8×10^{-3}
5	YMR 151-A	MA	AAB	1 : 1 : 2	52.16	859	1.10	1.1×10^{-3}
6	YMR 152-A	MA	AAB	1 : 1 : 4	63.7	1020	1.07	1.5×10^{-3}
7	YMR 157-A	MA	AAP	1 : 1 : 1	23.93	470	1.06	0.4×10^{-3}
8	YMR 158-A	MA	AAP	1 : 1 : 2	36	467	1.07	0.7×10^{-3}
9	YMR 159-A	MA	AAP	1 : 1 : 4	47.8	478	1.07	1.0×10^{-3}
10	YMR 164-A	MA	ABA	1 : 1 : 1	27	495	1.03	0.5×10^{-3}
11	YMR 163-A	MA	ABA	1 : 1 : 2	31.1	505	1.04	0.6×10^{-3}
12	YMR 162-A	MA	ABA	1 : 1 : 4	32.11	535	1.06	0.6×10^{-3}

[a] k_{app}, the slope of $\ln[M_o]/[M]$ versus time plot.

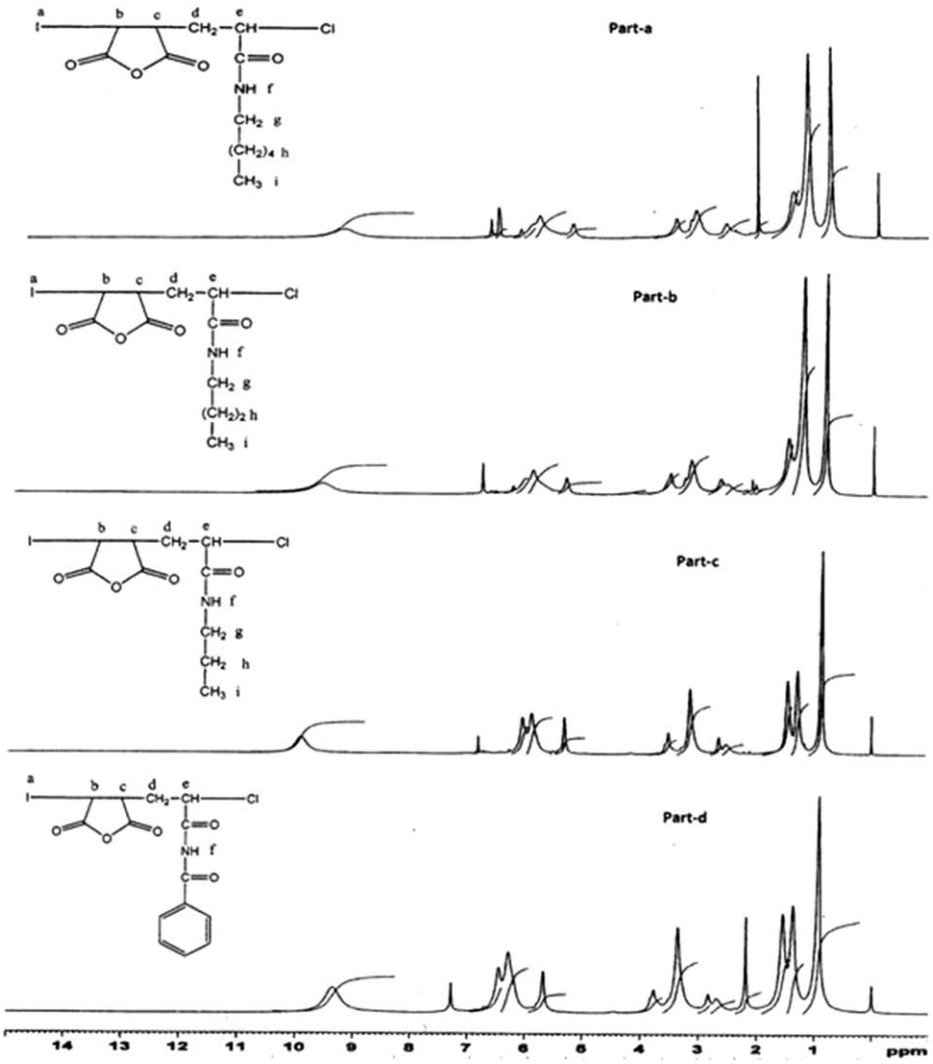

Figure 1. ^{1}H-NMR spectra of copolymers. From top: (a) AAH/MA copolymer; (b) AAB/MA copolymer; (c) AAP/MA copolymer; and (d) ABA/MA copolymer.

$CDCl_3$. Peaks located between 125 and 137 ppm are due to the benzene ring of the benzamide group. The carbonyls in the maleic anhydride and amide groups give peaks between 168 and 174 ppm.

Kinetics of Copolymerization

The new catalytic system, $FeCl_2$/SA, was successfully used in ATRP of maleic-anhydride copolymers. Well defined copolymers were obtained when o-xylene was used as the solvent at 140°C. When the molar ratio of $FeCl_2$/SA is 1:4, the polymerization was best controlled. The monomer conversion reached about 71 % corresponding to 1:4 [$FeCl_2$] to [SA] molar ratios for AAH/MA copolymer initiated by CPN whereas for the polymerization initiated by MCPN the conversion reached 52 % under similar condition. This can also be observed from the value of apparent rate constant (k_p^{app}) calculated from kinetic plot which is higher for (AAH/MA) copolymer initiated by CPN as compared to the system initiated by MCPN (Tables I and II). Therefore, this clearly shows that CPN is better initiator in comparison to MCPN for maleic-anhydride copolymerization system.

Figures 3–6(a) compares the polydispersities at varying $FeCl_2$/SA ratios. These indicate a broadening of the molecular weight distribution at the start of the reaction which reached about 1.22 to 1.20. It is obvious that the polydispersity index of the resulting polymers show a trend of decrease with the increase of polymerization conversion. It can also be seen from these figures that a broader polydispersity is obtained during the start of the reaction, but beyond this the PDI of the resulting polymers is narrow suggesting that the concentration of radicals in the reaction medium at the start of the reaction was too high. This could be due to the addition of initiator CPN or MCPN in incremental amounts over a time of 30 min. As the half life of CPN and MCPN at the reaction temperature was less than 30 min, it was exhausted within a short period and the polydispersity gradually decreased with time exhibiting the livingness of the reaction.

Figures 3–6(b) illustrate an approximately linear increase of molecular weight with conversion for all the system studied. On increasing the $FeCl_2$/SA ratio as expected we observe high molecular weight polymer and a best controlled reaction is

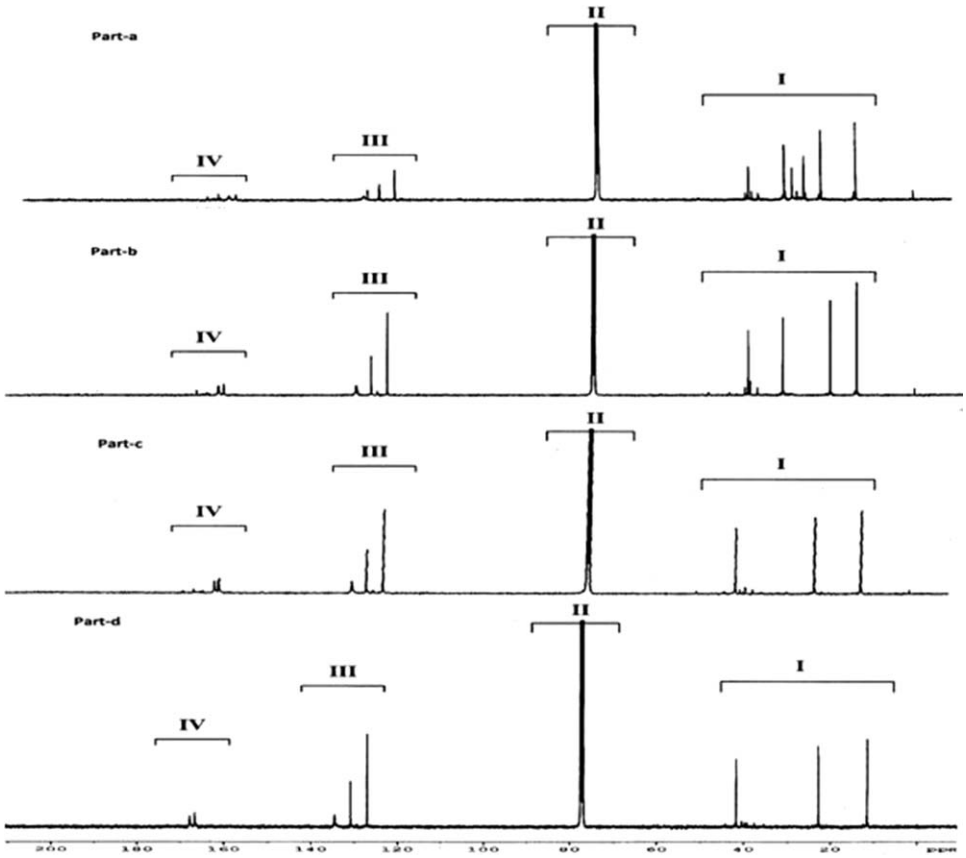

Figure 2. ^{13}C-NMR spectra of copolymers. From top: (a) AAH/MA copolymer; (b) AAB/MA copolymer; (c) AAP/MA copolymer; and (d) ABA/MA copolymer.

observed at $FeCl_2$/SA molar ratio of (1:4) which shows maximum conversion and the highest molecular weight, whereas on lowering the molar ratio up to $FeCl_2$/SA (1:1) the molecular weight and conversion decreases. The low molecular weight in the range of 495 – 598 in the case of (ABA/MA) copolymers could be due to the steric hindrance of the bulky benzene group in acryloylbenzamide monomer which impedes the rate of propagation.

The kinetic plots for the copolymerization shown from Figures 7–10 are quite linear indicating the steady state assumption holds. In addition there is a good correlation between the actual and theoretical values. Under these conditions, the polymerization showed fairly good living character.

Antiscaling Properties of Polymers (YMR-A Series)

YMR-A series polymers are good scale inhibitors as can be observed from the Figures 11 and 12, where they inhibit the deposition of calcium carbonate and calcium sulfate salts and shows inhibition efficiency at varying antiscalant concentration. Static scale inhibition tests[43–46] were conducted as per the standard NACE TM 0374-95 and ASTM D 1126-02. Briefly brines were prepared for $CaSO_4$ and $CaCO_3$ precipitation test as per standard NACE TM 0374 – 95. Anti-precipitation tests were conducted for a time period of 24 Hrs, pH – 10.45 and at a temperature of 70°C, as per the standard NACE TM 0374-95. Calcium concentrations are determined as per standard ASTM D1126-02.

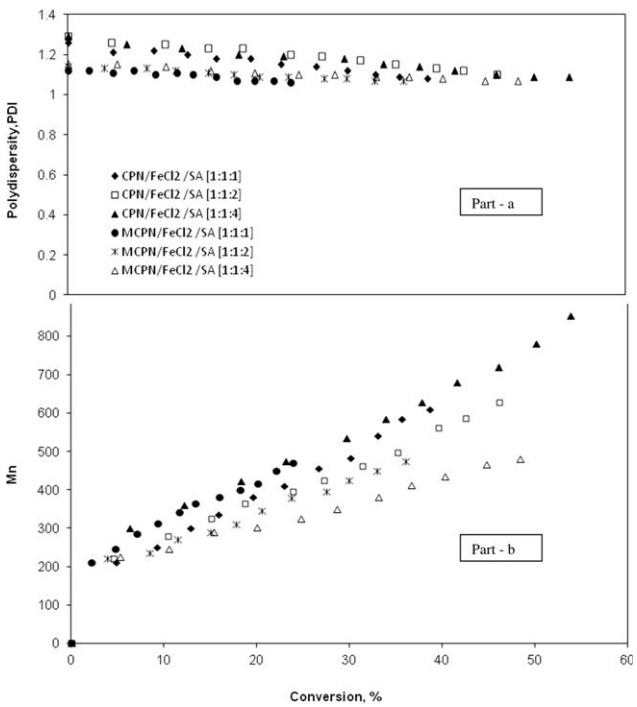

Figure 3. Plots showing dependence of (a) Polydispersity and (b) Number average molecular weight on conversion in the copolymerization of AAP and MA in o-xylene at different initiators.

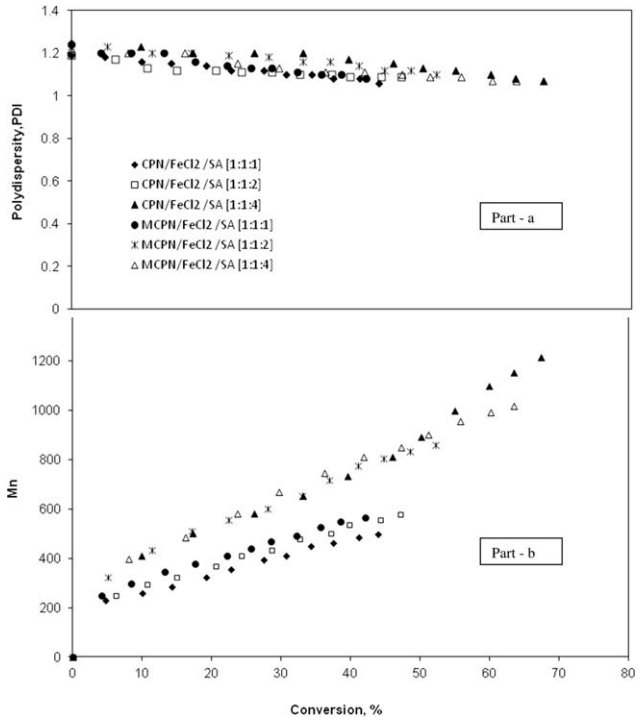

Figure 4. Plots showing dependence of (a) Polydispersity and (b) Number average molecular weight on conversion in the copolymerization of AAB and MA in o-xylene at different initiators.

YMR-A polymers are all highly effective inhibitors of $CaSO_4$ and $CaCO_3$ precipitation. $CaSO_4$ tests were conducted at 1, 2, 3, 5, and 7ppm of YMR-A polymers. Inhibition as far as 93.21 % is observed at 7 ppm level (Figure 11). Whereas for $CaCO_3$

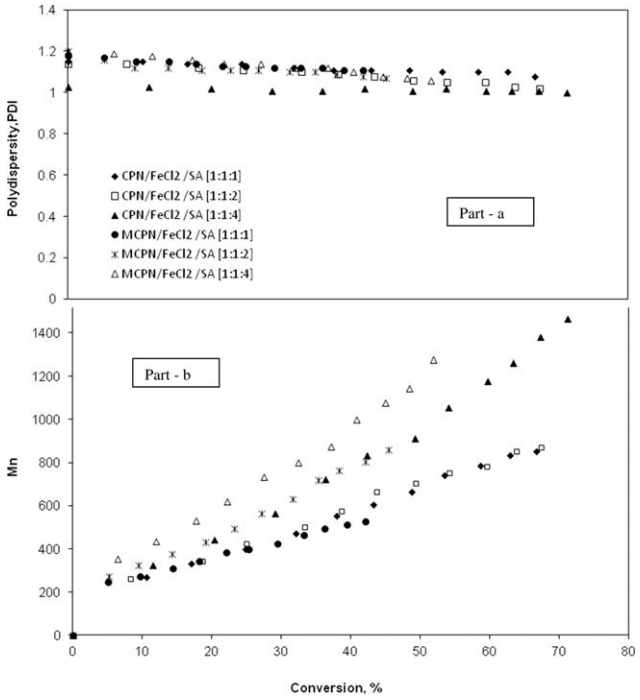

Figure 5. Plots showing dependence of (a) Polydispersity and (b) Number average molecular weight on conversion in the copolymerization of AAH and MA in o-xylene at different initiators.

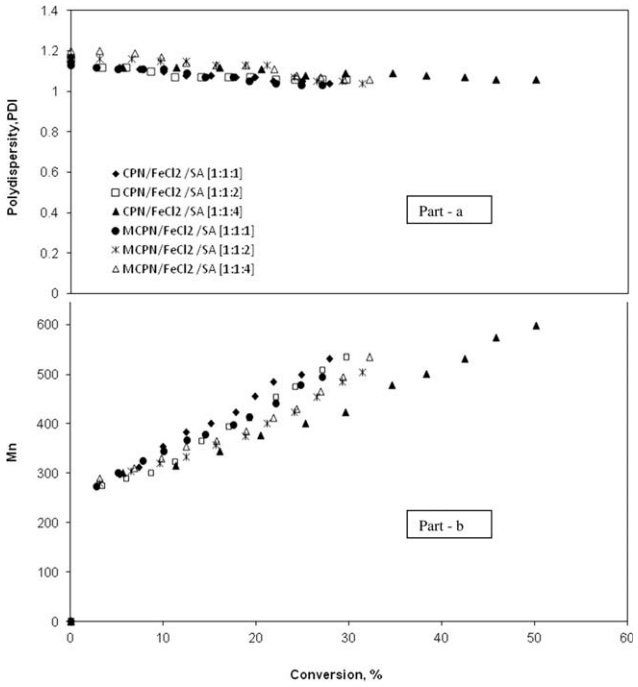

Figure 6. Plots showing dependence of (a) Polydispersity and (b) Number average molecular weight on conversion in the copolymerization of ABA and MA in o-xylene at different initiators.

precipitation tests were made with 1, 2, 3, and 5 ppm of YMR-A polymers. Inhibition as far as 99.33 % was observed (Figure 12) at 5 ppm level for all the n-alkylacrylamide/maleic anhydride copolymer. An increasing trend is observed in inhibition percent with molecular weight and reaches maximum at molecular weight range of 1020–1466 as observed in Figures 11 and 12. Percentage inhibition was calculated by using eq. (1) below:

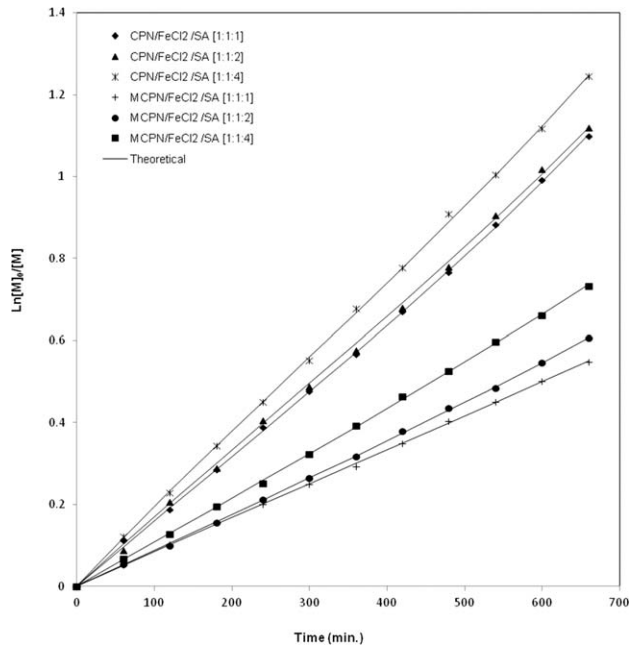

Figure 7. Kinetic plot of $\mathrm{Ln}[M]_0/[M]$ vs. time for the co-polymerization of AAH and MA in o-xylene at different initiators.

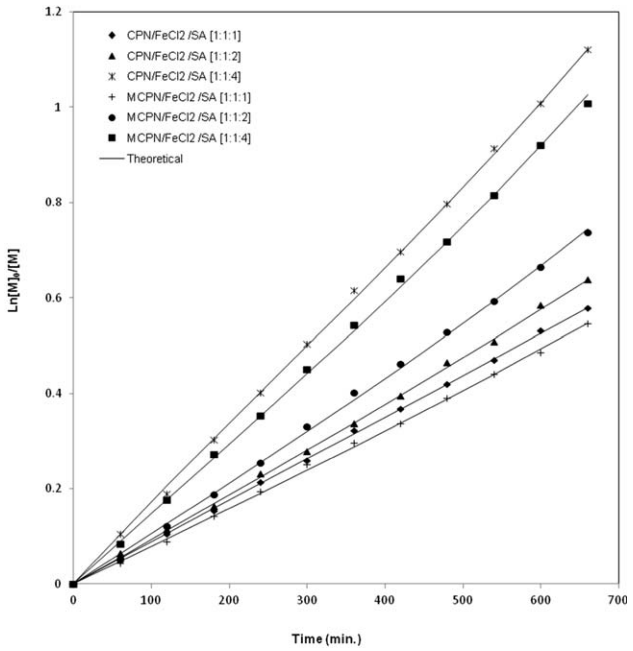

Figure 8. Kinetic plot of $\mathrm{Ln}[M]_0/[M]$ vs. time for the co-polymerization of AAB and MA in o-xylene at different initiators.

$$\%\ \text{inhibition} = \frac{[Ca^{2+}]_{\text{antiscalant}} - [Ca^{2+}]_{\text{blank}}}{[Ca^{2+}]_{\text{original}} - [Ca^{2+}]_{\text{blank}}} \times 100 \qquad (1)$$

where:

$[Ca^{2+}]_{\text{antiscalant}}$ = concentration of soluble Ca^{2+} in an antiscalant containing solution (mg/L)

$[Ca^{2+}]_{\text{original}}$ = concentration of soluble Ca^{2+} in original solution (mg/L)

$[Ca^{2+}]_{\text{blank}}$ = concentration of soluble Ca^{2+} in a blank solution (mg/L)

SEM Studies

The change of crystal habit, size and modifications brought about by YMR-A polymer addition, were examined through scanning electron microscope (SEM). The SEM photographs for the $CaCO_3$ and $CaSO_4$ with and without the presence of the polymer are presented in Figures 13 and 14. The crystal habit of calcium carbonate has at least three polymorphs: calcite, aragonite, and vaterite, depending on the temperature, pressure, substrate, etc. The vaterite crystals are usually formed at low temperature. The aragonite crystals are needle[49] and flower-like structures,[50] while the calcite crystals are block like[49] particles of cubic shape[50] or entangled rhombohedra[51]. In this study, crystals of calcite and aragonite are formed which can be observed in Figure 13(a), for Blank (effect of $CaCO_3$ crystal without the presence of polymer). We have studied the effect of YMR154-A on the calcite crystals and found that there is an alteration in crystal size [Figure 13(b)]. The SEM micrographs reveal that the scale deposit consists mainly of distorted crystals with rough rounded edges fused together and also sludge-like precipitates. There is a total disappearance of needle shape, block like structures of calcite and aragonite crystals.

The SEM photographs for $CaSO_4$ scales with and without the presence of YMR154-A polymers are presented in Figures 14(a,b). Among the three types of calcium sulfate crystals,[52] calcium sulfate dihydrate crystal was formed from the supersaturated solution at a temperature of 70°C without any additives. Calcium sulfate dihydrate crystals are thin tubular cells and needles exhibiting monoclinic symmetry.[53,54] The influences of YMR154-A polymer on the morphological changes of the scales were examined. In this study, SEM images show the absence of the tubular cell shaped $CaSO_4.2H_2O$ with reduced size. Besides we also observe reduced crystallinity with spongy deposits is formed.

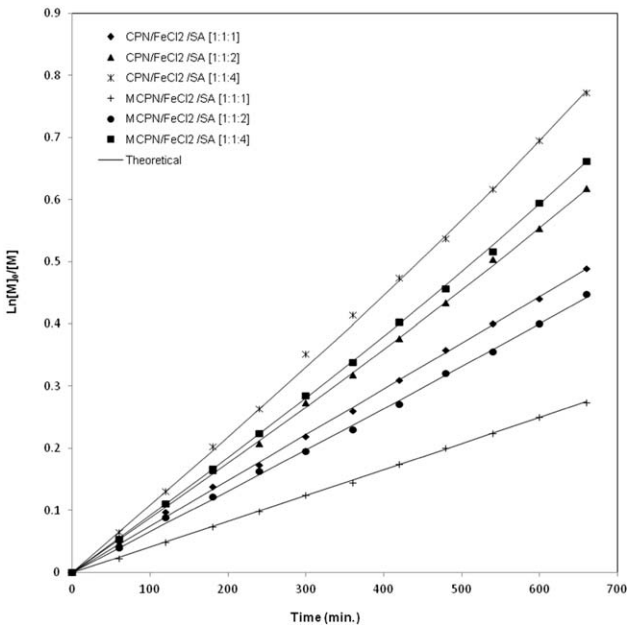

Figure 9. Kinetic plot of $\mathrm{Ln}[M]_0/[M]$ vs. time for the co-polymerization of AAP and MA in o-xylene at different initiators.

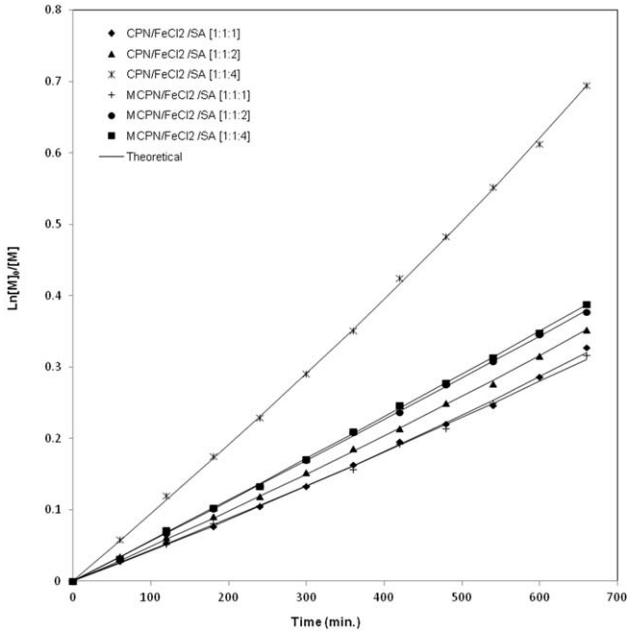

Figure 10. Kinetic plot of $\mathrm{Ln}[M]_0/[M]$ vs. time for the co-polymerization of ABA and MA in o-xylene at different initiators.

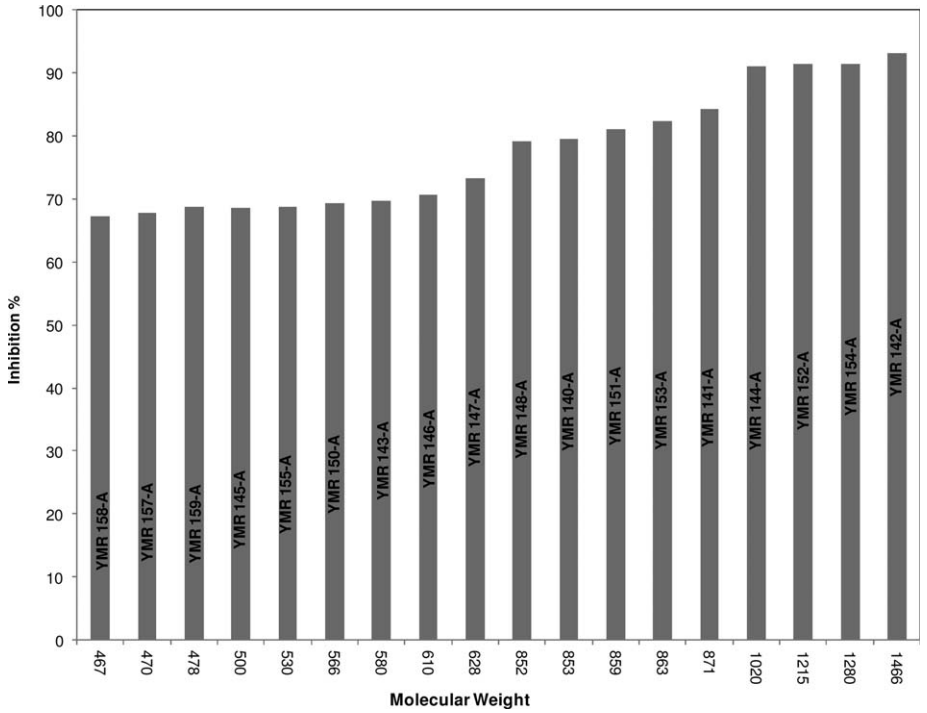

Figure 11. Plot showing scale inhibition % with varying molecular weight range for different YMR-A series polymers at 7 ppm level of the antiscalant concentration for $CaSO_4$ scales.

During crystal growth, inhibitor molecules are adsorbed at different concentrations onto various types of crystal faces since each type of face has a different surface lattice structure. Thus, the inhibitor has different distribution on the adsorption sites. Different degrees of growth retardation for each type of crystal face result in alteration in crystal shape

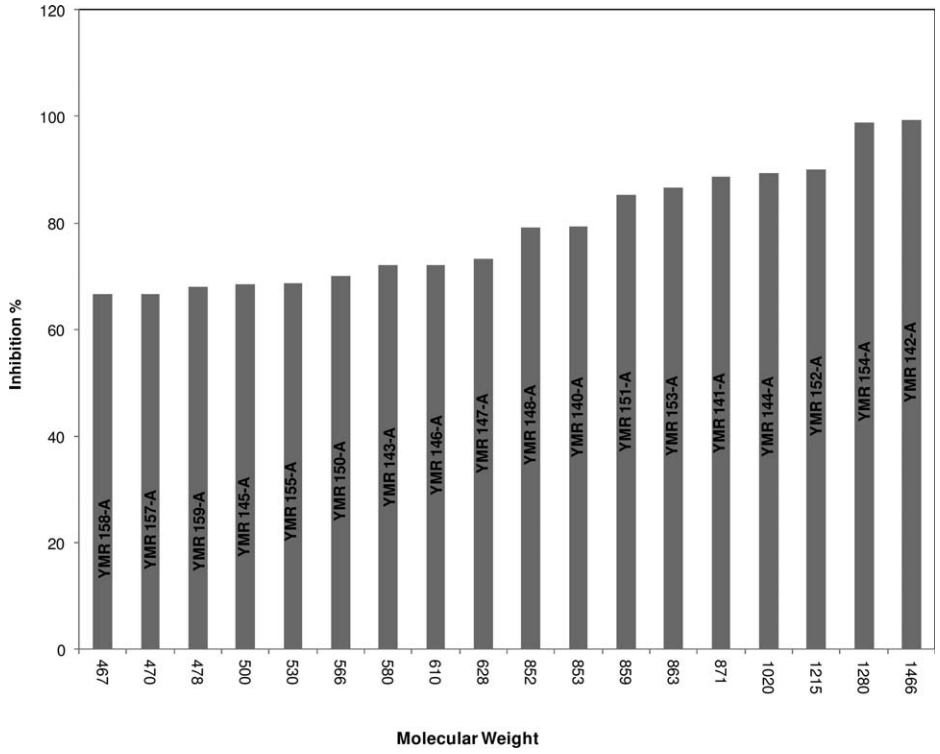

Figure 12. Plot showing scale inhibition % with varying molecular weight range for different YMR-A series polymers at 5 ppm level of the antiscalant concentration for $CaCO_3$ scales.

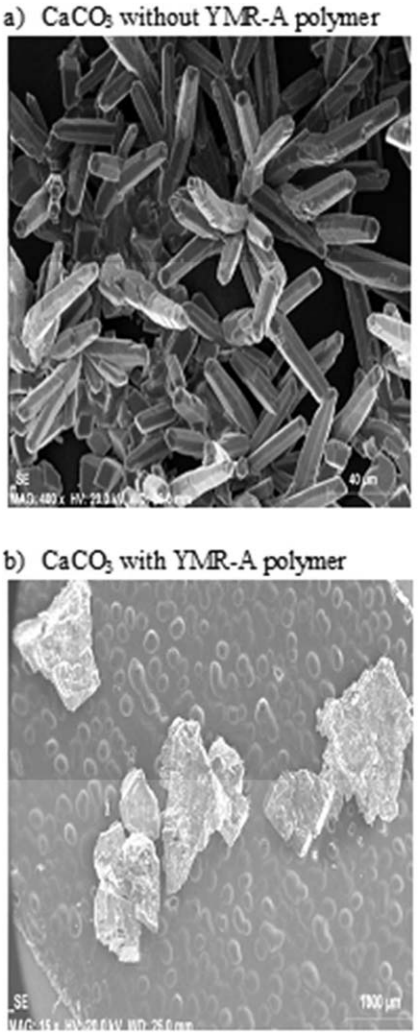

Figure 13. SEM images of $CaCO_3$ deposits in the absence (a) and in the presence (b) of YMR154-A polymer.

during outgrowth. The habit-modifying influence of an inhibitor can be so pronounced that one or more crystal faces either appear or disappear with advancing outgrowth of the crystals. The crystal morphology is then changed, that is, the crystal cannot grow normally in accordance with an array of crystal lattices strictly, causing the crystal to become distorted or increasing the internal stress of crystals. Increase in stress could result in crystal fractures and prevention of deposition of microcrystalline.[22,45]

CONCLUSIONS

Antiscalants are one of the most valuable commercial polymers and have been used widely across the world as scale inhibitors. Improving their properties by controlling their molecular weight is of great significance. Various kinds of antiscalants have been prepared by us through free radical polymerization. Therefore, in our present work, the new catalytic system, $FeCl_2$/SA, was successfully used in ATRP of maleic-anhydride copolymers (YMR-A series). Well defined copolymers having a low molecular weight in the range of 500–1466 and a polydispersity of 1–1.11 were obtained. The increase of polymerization rate and Mn of obtained polymer were observed with the increase of the molar ratio of $FeCl_2$/SA up to (1:4). The monomer conversion reached about 71 % corresponding to 1:4 [$FeCl_2$] to [SA] ratios for (AAH/MA) copolymer initiated by CPN whereas for the polymerization initiated by MCPN the conversion only reached 51.9 % under similar condition. Therefore this clearly shows that CPN is better initiator in comparison to MCPN for maleic-anhydride copolymerization system.

YMR-A series polymers are highly effective scale inhibitors and the inhibition ability on the calcium carbonate scale is much higher, even with 5 ppm dosage level the efficiency is around 99.33 % at pH 10.45 and temperature 70°C. For calcium sulfate scales the inhibition efficiency is little lower than $CaCO_3$ and 99.9 % inhibition is observed at 9 ppm level. Besides with increase in molecular weight from 500 to 1466 the inhibition efficiency increases.

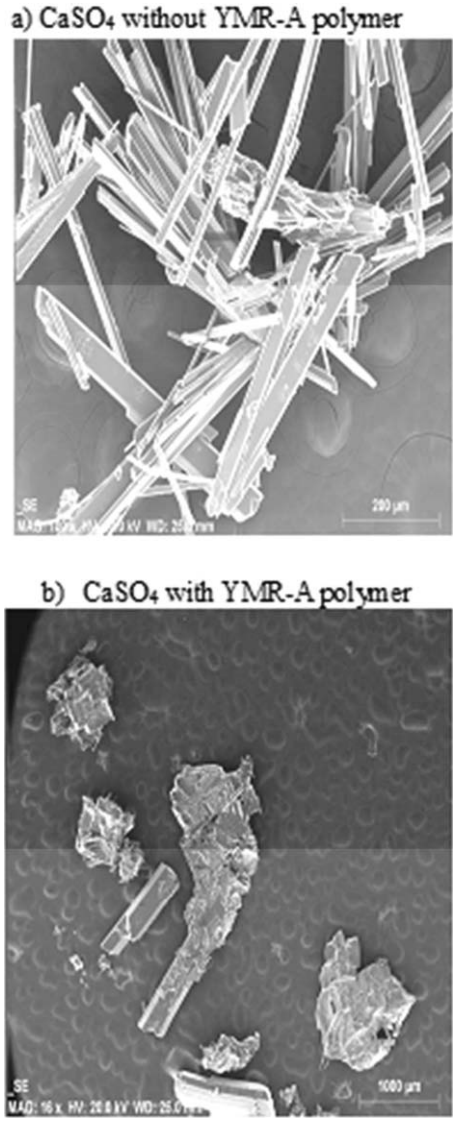

Figure 14. SEM images of $CaSO_4$ deposits in the absence (a) and in the presence (b) of YMR154-A polymer.

REFERENCES

1. Ketrane, R.; Saidani, B.; Gil, O.; Leleyter, L.; Baraud, F. *Desalination* **2009**, *249*, 1397.
2. Demadis, K. D.; Mavredaki, E.; Stathoulopoulou, A.; Neofotistou, E.; Mantzaridis, C. *Desalination* **2007**, *213*, 38.
3. Wu, Z.; Davidson, J. H.; Francis, L. F. *J. Colloid Interface Sci.* **2010**, *343*, 176.
4. Greenlee, L. F.; Testa, F.; Lawler, D. F.; Freeman, B. D.; Moulin, P. *Water Res.* **2010**, *44*, 2957.
5. Chesters, S. P. *Desalination* **2009**, *238*, 22.
6. Li, H.; Liu, W.; Qi, X. *Desalination* **2007**, *214*, 193.
7. Tzotzi, C.; Pahiadaki, T.; Yiantsios, S. G.; Karabelas, A. J.; Andritsos, N. *J. Membrane Sci.* **2007**, *296*, 1-2, 171.
8. Kumar, T.; Vishwanatham, S.; Kundu, S. S. *J. Pet Sci. Eng.* **2010**, *71*, 1.
9. Ghizellaouia, S.; Euvrardb, M.; Ledionc, J.; Chibania, A. *Desalination* **2007**, *206*, 185.
10. Zhang, Y.; Jihuai, W. U.; Sancun, H. A. O.; Minghua, L. I. U. *Chinese J. Chem. Eng.* **2007**, *15*, 600.
11. Al-Deffeeri, N. S. *Desalination* **2007**, *204*, 423.
12. Duffy, J. R.; Higgins, M. A.; Schiller, A. M.; Song, D. S.; Witschonke, C. R. US Patent 4085045 (**1978**).
13. Cenergy, M. L.; Griffith, D. F.; Hobbs, G. W. M.; US Patent 5044439 (**1991**).
14. Senthilmurugan, B.; Ghosh, B.; Sanker, S. *J. Indust. Eng. Chem.* **2011**, *17*, 415.
15. Jones, I. T.; Graham, G.; Finan, M. A. UK Patent GB1414918 (**1975**).
16. Jones, I. T.; Richardson, N.; Harris, A. US Patent 3810834.
17. Libutti, B. L.; Knudsen, J. G.; Mueller R. W. Corrosion/841, Paper No. 119, (Houston, TX: NACE International, **1984**).
18. Master W. F.; Amjad Z.; Corrosion/88, Paper No. 11, (Houston, TX: NACE International, **1988**).
19. Amjad Z.; Corrosion/96, Paper No. 230, (Houston, TX: NACE International, **1996**).
20. Moulay S.; Boukherissa M.; Abdoune F.; Benabdelmoumene F. Z. *J. Iranian Chem. Soc.* **2005**, *2*, 212.
21. Weijnen M. P. C.; Rosmalen, van G. M. *Desalination* **1985**, *54*, 239.
22. Yang, Q. F.; Liu, Y. Q.; Gu, A. Z.; Ding, J.; Shen, Z. Q. *J. Colloid Interface Sci.* **2001**, *240*, 608.
23. Xyla A. G.; Mikroyannidis, J.; Koutsoukos, P. G. *J Colloid Interface Sci.* **1992**, *153*, 537.
24. Ghani, A. I.; Dalvi, M. N.; Kither, M.; Saad, Al-S.; Sahul, K.; Al-Rasheed, R. *Desalination* **1999**, *123*, 177.
25. Al-Zahrani, S. G.; Al-Ajlan A. M.; Al-Jardan, A. M. Using different types of antiscalants at the Al-Jubail power and desalination plant in Saudi Arabia, 6th IDA World Congress, Yokohoma, **1993**.
26. Al-Saleh, S.A.; Khan, A. R. *Desalination* **1994**, *97*, 87.
27. Hamed, O. A.; Al-Sofi, M. A. K.; Mustafa, G. M.; Dalvi, A. G. *Desalination* **1999**, *123*, 185.
28. Al-Roomi, Y. M.; Hussain, K. F. *J. Appl. Polym. Sci.* **2006**, *102*, 3404.
29. Al-Roomi, Y. M.; Hussain, K. F. *Polym. Bull.* **2005**, *55*, 81.
30. Al-Roomi, Y. M.; Hussain, K. F.; Riazi, M. R. *J. Pet Sci. Technol.* **2012**, *81*, 151.
31. Chen, H.; Ying, L.; Liu, D.; Tan, Z.; Zhang, S.; Zheng, M.; Qu, R. *Mater. Sci. Eng. C* **2010**, *30*, 4, 605.
32. Dhyaneshwar, V. P.; Sane, P. S.; Wadgaonkar, P. P. *React. Funct. Polym.* **2010**, *70*, 12, 931.
33. Pietrasik, J.; Tsarevsky, N. V. *Eur. Polym. J.* **2010**, *46*, 12, 2333.
34. Liu, Y.; Chen, M.; Hsu, K. *React. Funct. Polym.* **2009**, *69*, 424.
35. Matyjaszewski, K.; Wei, M.; Mcdermott, N. E.; Xia, J. *Macromolecules* **1997**, *30*, 8161.
36. Gibson, V. C.; O'Reilly, R. K.; Wass, D. F.; White, A. J.; Williams, D. J. *Macromolecules* **2003**, *36*, 2591.
37. O'Reilly, R. K.; Gibson, V. C.; White, A. J.; Williams, D. J. *J. Am. Chem. Soc.* **2003**, *125*, 8450.
38. O'Reilly, R. K.; Gibson, V. C.; White, A. J. P.; Williams, D. *J. Polyhedron* **2004**, *23*, 2921.
39. Ibrahim, K.; Yliheikkila, K.; Abu-Surrah, A.; Lofgren, B.; Lappalainen, K.; Leskela, M.; Repo, T.; Seppala. *J. Eur. Polym. J.* **2004**, *40*, 1095.
40. Cao, J.; Chen, J.; Zhang, K. D.; Shen, Q.; Zhang, Y. *Appl. Catalysis-A* **2006**, *311*, 76.
41. Xue, Z.; Noh, S. K.; Lyoo, W. S. *J. Polym. Sci. Part A: Polym. Chem.* **2008**, *46*, 2922.
42. Hou, C.; Ying, L.; Wang, C. *J. Appl. Polym. Sci.* **2006**, *99*, 1050.
43. Shakkthivel, P.; Ramesh, D.; Sathiyamoorthi, R.; Vasudevan, T. *J. Appl. Polym. Sci.* **2005**, *96*, 1451.
44. Ling, L.; Zhou, Y.; Huang, J.; Yao, Q.; Liu, G.; Zhang, P. *Desalination* **2012**, *304*, 33.
45. Hui, F.; Liu, D. *Desalination* **2012**, *304*, 1.
46. Tang, Y.; Yang, W.; Yin, X.; Liu, Y.; Yin, P. *Desalination* **2008**, *228*, 55.
47. Pouchert, J. C. The Aldrich library of NMR spectra, Ed.-II, volume 1 and 2.
48. Pouchert, J. C.; Behnke, J. The Aldrich library of ^{13}C and ^{1}H FT-NMR spectra, Ed.-I, volume 1 and 3.
49. Ledion, J.; Leory, P.; Labbe, I. P. *TSML eau* **1985**, *80*, 323-328.
50. Deslouis, C.; Festy, D.; Gil, O.; Ruis, G.; Touzain, S.; Tribollet, B. *Electrochim. Acta* **1998**, *43* (12-13), 1891.
51. Gabrielli, C.; Keddam, M.; Perrot, H.; Khalil, A.; Rosset, R.; Zidoune, M. *J. Appl. Electrochem.* **1996**, *26*, 1125.
52. Shakkthivel, P.; Saathiyamoorthi, R.; Vasudevan, T. *Desalination* **2004**, *164*, 111.
53. Salmon, J. C. Polymer Materials Encyclopedia **1996**, CRC Press, Boca Raton, 7587.
54. Austin, A. E.; Miller, J. F.; Vaughan, D. A.; Kircher, J. F. *Desalination* **1975**, *16*, 345.